Effects of slit shapes on the flashback limits of premixed hydrogen slit burners

F. Fruzza*[1], H. Chu[2], R. Lamioni[1], T. Grenga[3], C. Galletti[1], and H. Pitsch[2]

[1]Dipartimento di Ingegneria Civile e Industriale, University of Pisa, Pisa 56126, Italy
[2]Institute for Combustion Technology, RWTH Aachen University, Aachen 52056, Germany
[3]Faculty of Engineering and Physical Science, University of Southampton, Southampton SO17 1BJ, UK

Abstract

With a growing interest in hydrogen as a clean fuel for providing heat in residential and commercial sectors, the development of new designs for end-user devices is becoming increasingly necessary to ensure both efficiency and safety. In this work, we use 3D simulations to investigate the effects of slit shape and dimensions on the flashback limits for hydrogen premixed flames in perforated burners, typically employed in end-user devices such as condensing boilers. We compute flashback velocities for different slit lengths and widths and analyze the results in terms of the physical mechanisms involved.

Introduction

In the context of the massive incorporation of renewable resources requested by the EU Green Deal [1], green hydrogen has emerged as a valid candidate to boost decarbonization in several sectors, including heating for residential and commercial buildings. Domestic end-user devices are typically equipped with perforated cylindrical or flat burners which inject a premixed mixture into the combustion chamber and generate short-length flames that fit in the compact volume between the burner and the heat exchanger coils. However, hydrogen exhibits very different physical properties compared with natural gas, which is currently used in these devices. The laminar flame speed of H_2-air mixtures is around six times higher than that of natural gas at stoichiometric conditions, and the hydrogen flame thickness is smaller than that of methane. Moreover, the effective Lewis number of lean air/hydrogen mixtures is significantly smaller than those of air/natural gas, which is around unity. These effects significantly change the combustion characteristics and complicate the stabilization of premixed H_2 and H_2/CH_4 flames. Since the perforated burners equipped on end-user devices, e.g. condensing boilers, typically work in premixed conditions, these effects have to be taken into account in the design process to avoid safety issues and low performance related to high burner temperatures and flashback. Flashback limits of H_2 and H_2/CH_4 in domestic burners have been investigated experimentally by de Vries et al. [2] and Aniello et al. [3], founding a strong correlation between flashback regimes and burner plate temperatures. Pers et al. [4] evaluated experimentally the impact of wall temperature on flashback for H_2-enriched CH_4-air flames by investigating the possibility of autoignition as a flashback initiation mechanism. Vance et al. [5] studied numerically the flashback limits of premixed hydrogen flames in 2D configurations emulating multi-slit burners, first including the conjugate heat transfer between the flame and the burner plate, and investigating the effects of the geometry parameters involved on the flashback limits. However, given the complexity of the phenomena involved, a 2D model might not be able to capture the actual flashback dynamics occurring in a real burner, resulting in an inaccurate estimation of flashback velocities. Furthermore, an analysis of the effects of the three-dimensional slit shape, such as its length and width, on the flashback dynamics is still lacking in the literature: that could provide useful information for burner design, as it needs to be completely revised in order to use hydrogen safely. In this work, we use 3D numerical simulations to investigate the effects of the shape of the slits on the flashback limits of a H_2-air flames with an equivalence ratio of $\phi = 0.6$. The numerical model encompasses the conjugate heat transfer between the flame and the burner plate to address the temperature increase of the burner plate, occurring when approaching flashback limits, to include the effects of the high wall temperatures on flashback.

Configuration and numerical methods

In this study, 3D simulations of flashback of premixed hydrogen flames were performed using ANSYS-FLUENT 22.1 [6]. We considered a 3D configuration representing a single hole or a single slit with rounded ends of different shapes and sizes, emulating a portion of a real burner plate typically used in domestic condensing boilers. The 3D configuration is shown in Figure 1: the slit width is denoted by W, while the distance between two adjacent slits is denoted by D. The distance between the centers of the round ends of the slit is denoted by L, such that $L = 0$ corresponds to a circular hole of diameter W. The burner plate thickness is $T = 0.6\,\text{mm}$ for all cases. For any variation of W and L, the distance between the slits D is varied in order to fix the porosity of the burner, defined as A_{slit}/A_{tot}. Due to the symmetries of the problem, the computational domain can be reduced to a quarter of the entire slit, with symmetry boundary conditions on the symmetry planes. Since we want to simulate a slit being part

*Corresponding author: filippo.fruzza@phd.unipi.it

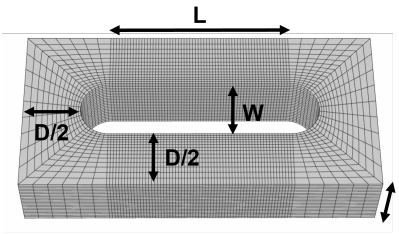

Figure 1: 3D configuration of a slit.

of a group in a multi-slit burner, symmetry boundary conditions are imposed on the external edges of the domain as well, to consider the interaction with the adjacent slits. The computational domain is shown in Figure 2, where the solid zone corresponding to the burner plate is shown below. The boundary conditions are indicated in red. The fluid domain extends enough both downstream ($H_{out} = 8\,\text{mm}$) and upstream ($H_{in} = 4\,\text{mm}$) of the solid. For all cases investigated in this work,

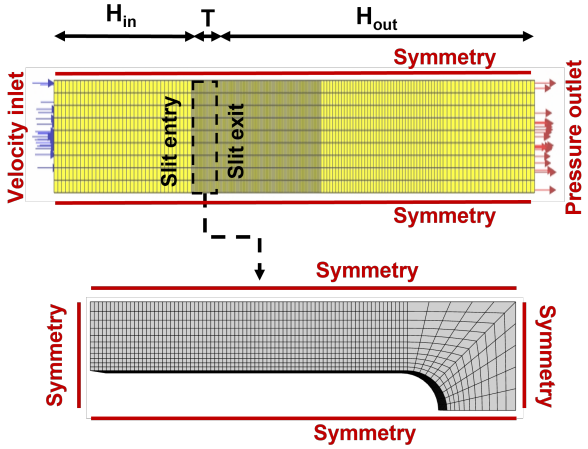

Figure 2: Computational domain.

an H_2-air mixture with an equivalence ratio of $\phi = 0.6$ was used. Uniform velocity and uniform temperature of $T_u = 300\,\text{K}$ are set at the inlet, and a pressure outlet with $p = 1\,\text{atm}$ is imposed at the outlet. A no-slip boundary condition is given for the velocity at the fluid-solid interface. We note that no thermal boundary conditions are needed at the fluid-solid interface since the heat fluxes are computed directly as described below.

For the fluid, transport equations of mass, momentum, energy, and chemical species are solved on a structured grid, with characteristic cell size in the reaction region of $\Delta x = 25\,\mu\text{m} \simeq \delta_F/13$. The gas phase is modeled as an ideal gas. We use detailed chemistry employing a reduced mechanism with 9 chemical species and 22 reactions, derived from the Kee-58 skeletal mechanism [7]. Full multicomponent diffusion is modeled through generalized Fick's law coefficients derived by the Maxwell-Stefan equations [6, 8, 9]. Soret diffusion is modeled using an empirically-based formula provided by Kuo [10]. Radiation is modeled by means of the gray Discrete Ordinates (DO) method [11], assuming the emissivity of the fluid-solid interface to be 0.85 [5]. The burner plate is modeled as a solid with the properties of the stainless steel typically used for this kind of burner, with density $\rho_s = 7719\,\text{kg}\,\text{m}^{-3}$, specific heat $C_{p,s} = 461.3\,\text{J}\,\text{kg}^{-1}\,\text{K}^{-1}$, and thermal conductivity $k_s = 22.54\,\text{W}\,\text{m}^{-1}\,\text{K}^{-1}$. Inside the solid domain, we solve the energy equation. The conjugate heat transfer (CHT) between the fluid and the solid zones is modeled to consider the interaction between the flame and the burner plate. The CHT is modeled using Fourier's Law to compute the heat flux through the fluid-solid interface [6]. The reference laminar flame speed ($S_L = 1.000\,\text{m/s}$) and flame thickness ($\delta_F = 0.345\,\text{mm}$), which we use to normalize the quantities in this study, correspond to that of a 1D unstretched laminar flames with the same thermodynamic conditions at the inlet, i.e., $\phi = 0.6$, $T_u = 300\,\text{K}$, and $p = 1\,\text{atm}$.

Solution methodology

We set steady-state simulations using the pressure-based coupled algorithm available in ANSYS-FLUENT 22.1 [6], using a second-order upwind scheme. Given the large number of simulations required for the parametric variations investigated in this study, a steady-state approach is needed for reasons of computational cost. We start from a stable flame with a high inlet velocity, then the inlet velocity is decreased by a step of $\Delta V_{in} = 0.1\,\text{m/s}$ to find a new configuration of the flame. This procedure is repeated systematically until a critical velocity is reached for which a stable configuration of the flame is not found: here, we assume that flashback has occurred. When approaching the flashback limit, we employ an additional refinement of $\Delta V_{in} = 0.01\,\text{m/s}$. This method allows us to estimate the flashback velocity for each case. We define the *cold-flow* bulk velocity at the slit entry as

$$V_S = \frac{A_{tot}}{A_{slit}} V_{in}, \tag{1}$$

where V_{in} is the uniform inlet velocity. V_S is the velocity we would have for a cold flow, i.e., neglecting the density variations of the mixture due to the high burner plate temperatures. We point out that the choice of fixing the porosity of the burner plate A_{slit}/A_{tot} allows V_S to be directly related to the total power of the burner, with equal slit velocities for different slits implying equal power to be supplied to the burner. We define the flashback velocity V_{FB} as V_S, defined in Eq. 1, when flashback occurs

$$V_{FB} = V_S|_{FB} = \frac{A_{tot}}{A_{slit}} V_{in}|_{FB}\,. \tag{2}$$

Figure 3 shows an example of the solution procedure, where we plot temperature and H_2 consumption rate profiles for a hole with diameter $W = 0.5\,\text{mm}$ and porosity $A_{slit}/A_{tot} = 0.3$ on a section through the center line for decreasing inlet velocities. It can be seen that by decreasing the inlet velocity, the flame approaches the

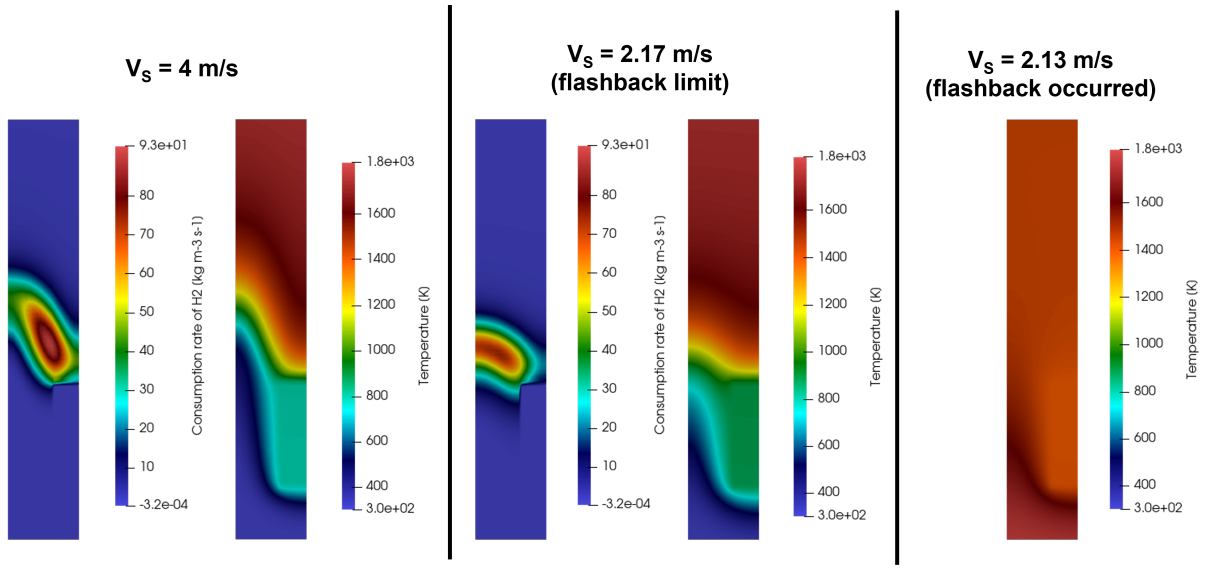

Figure 3: Temperature and H_2 consumption rate profiles for decreasing inlet velocity on a section of a hole with diameter $W = 0.5\,\text{mm}$ and porosity $A_{slit}/A_{tot} = 0.3$.

hole entry, increasing the burner plate temperature, until a stable configuration is not found with the flame flashing back into the hole.

To verify the steady-state approach and the estimated flashback velocities, transient simulations were performed on a domain representing the entire slit. We use the PISO solver with a time step of $\Delta t = 1\,\mu\text{s}$. Since the characteristic time scales of the reactive flow in the fluid domain and that of the heat conduction inside the solid domain are dramatically different, a uniform time step across the entire computational domain is not feasible due to computational cost. Therefore we applied a different time step for the solid zone, with $\Delta t_s = 10^4 \Delta t$. The uniqueness of the solution in the stable regimes and the consistency of the flashback velocities have been proven by using different solid time steps of 0.01 ms, 0.1 ms, 1 ms, 10 ms. No variations in the burner plate temperatures and in the estimated flashback velocity were observed. As test cases, we use a hole with diameter $W = 0.5\,\text{mm}$ and a slit with width $W = 0.5\,\text{mm}$ and length $L = 2\,\text{mm}$, both with porosity $A_{slit}/A_{tot} = 0.3$. In Figure 4, we show the volume-averaged burner plate temperature T_B as a function of the velocity at the slit entry V_S for the hole and the slit using the steady-state and the transient approaches: the last point on the left of each curve represents the flashback limits. It can be seen that the two methods are consistent: the steady-state approach is able to reproduce the correct burner plate temperatures and flashback velocities. Since the stationary approach is computationally much more efficient than the transient one (nearly 20 times faster), we use the former for estimating flashback velocities over a wide range of parameters as described below.

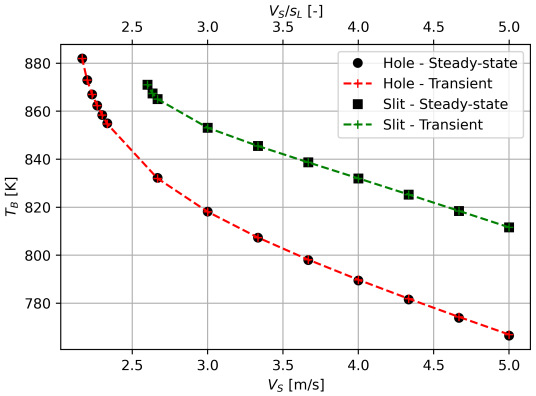

Figure 4: Burner plate temperature as a function of V_S for a hole and a slit, computed with the steady-state and the transient approaches.

Effect of slit length

To analyze the effect of the slit length L on the flashback limits, we employ the methodology described above to compute flashback velocities for different slits with $L = 0\,\text{mm}$ (hole), 1 mm, 2 mm, 4 mm, and 8 mm, keeping fixed the width $W = 0.5\,\text{mm}$ and the porosity $A_{slit}/A_{tot} = 0.2$. Longer slits are not investigated because they are not practically relevant for real burners. In Figure 5, we show the volume-averaged burner plate temperature T_B as a function of the velocity at the slit entry V_S for the different slits: the last point on the left of each curve is the flashback limit V_{FB} for the corresponding case. In Figure 6, we show the flashback velocity as a function of the slit length L. It can be seen that for $L > 1\,\text{mm}$, the burner plate temperature shows a weak dependence on the slit length, being lower for longer slits at the same slit velocity. Moreover, the flashback velocity approaches an almost constant value, $V_{FB} \simeq 3.3\text{-}3.4\,\text{m/s}$. The $L = 0$ case, corresponding to a hole, behaves differently, having lower burner plate temperatures: for instance, at $V_S = 5\,\text{m/s}$, T_B is decreas-

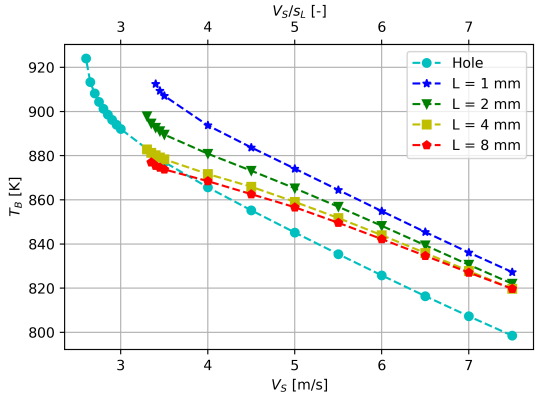

Figure 5: Burner plate temperature as a function of V_S for slits with different lengths. The case $L = 0$ corresponds to a hole.

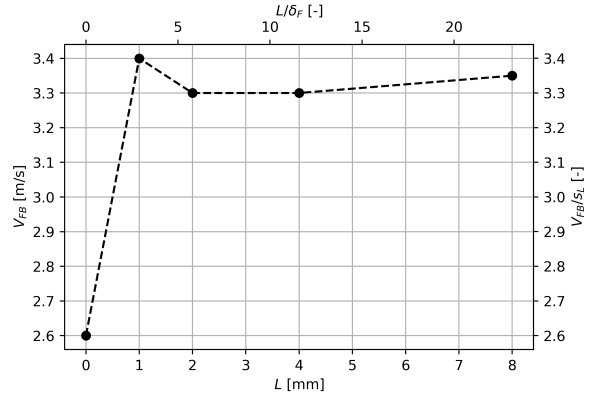

Figure 6: Flashback velocity as a function of slit length.

ing for increasing L, ranging from 1 mm to 8 mm, while T_B for $L = 0$ mm is lower than $L = 1$ mm. Moreover, the hole shows a significantly lower flashback velocity $V_{FB} = 2.6\,\mathrm{m/s}$. This nonlinear behavior when decreasing the slit length approaching a hole could be related to different flame-wall interaction mechanisms due to a more enclosed geometry and to preferential diffusion effects related to curvature. However, further investigation is needed to understand the details of the phenomenon.

To explain why we observe an almost constant flashback velocity for slits with $L > 1$ mm, a better understanding of the flashback dynamics is needed. In Figure 7, we show a snapshot of the transient simulation for a slit with $L = 2$ mm, corresponding to the instant when the flashback is initiated. We define a progress variable as $C = 1 - X_{H_2}/X_{H_2,u}$, where X_{H_2} is the H_2 molar fraction and $X_{H_2,u}$ is its value in the unburnt mixture, and we plot the iso-surface corresponding to $C = 0.5$. We also show the burner plate geometry as a reference. It can be seen that flashback is initiated at the ends of the slit. This phenomenon can explain why the length of the slit does not affect the flashback limit, as we expect the flashback to be always initiated at the slit ends, which have the same geometry regardless of the length of the slit. Nevertheless, further investigation is needed to better understand the mechanisms by which flashback occurs at the slit ends.

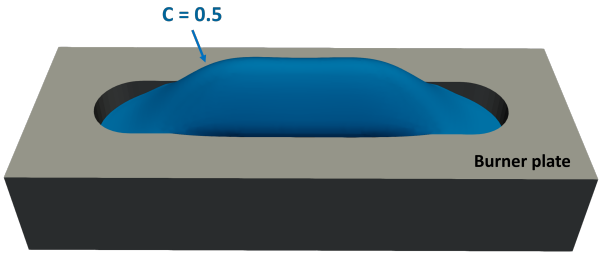

Figure 7: Snapshot of the transient simulation for a slit with $L = 2$ mm and $W = 0.5$ mm, corresponding to the instant when flashback is initiated. We plot an iso-surface of progress variable corresponding to $C = 0.5$. The burner plate geometry is included as a reference.

Effect of slit width

To investigate the effect of the width W on the flashback limits, we compute flashback velocities for slits with fixed length $L = 2$ mm and different widths, and for holes with different diameters. The porosity is kept fixed at $A_{slit}/A_{tot} = 0.2$ for all cases. In Figure 8, we show the volume-averaged burner plate temperature T_B as a function of the velocity at the slit entry V_S for the different slits. In Figure 9, we show the flashback velocity as a function of the slit width W. It can be seen that the burner plate temperatures increase when increasing the slit width, and the flashback velocity V_{FB} shows an almost linear dependence on W in the investigated range. In order to better investigate this behavior, we plot flow temperature and flow velocity profiles along a line going from the center of the round slit end to the burner wall, perpendicular to the longest axis and located halfway between the entrance and the exit of the slit, as shown in Figure 10. The temperature and velocity profiles for the limit cases $W = 0.4$ mm and $W = 0.8$ mm, with fixed $V_S = 6\,\mathrm{m/s}$, are shown in Figure 11, where the red vertical line corresponds to the burner wall position. For $W = 0.4$ mm, the two symmetrical thermal boundary layers merge at the center of the

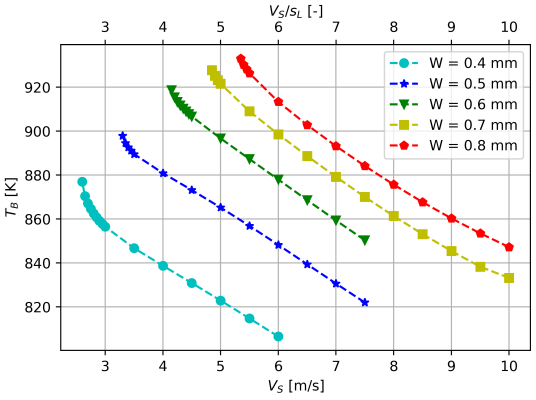

Figure 8: Burner plate temperature as a function of V_S for slits with $L = 2$ mm and different widths W.

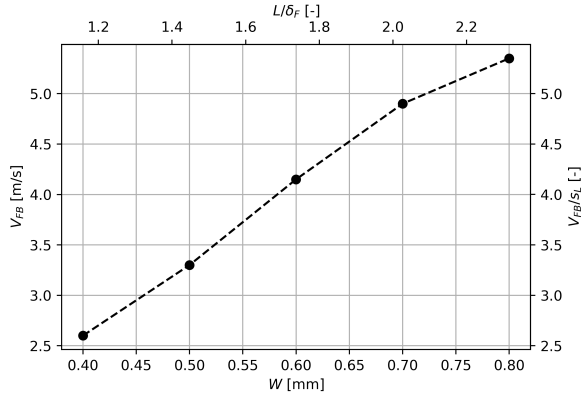

Figure 9: Flashback velocity as a function of the slit width W.

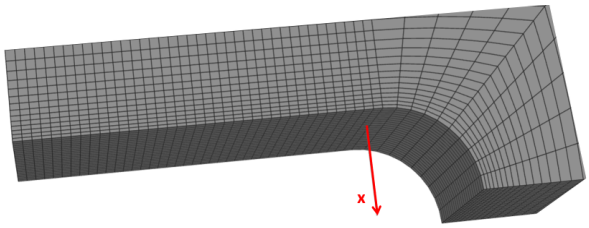

Figure 10: x axis for temperature and velocity profiles shown on the 3D geometry.

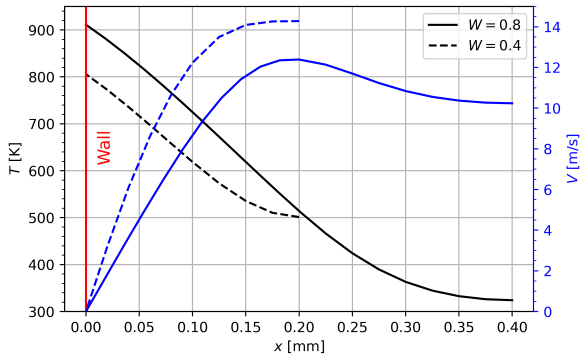

Figure 11: Flow temperature and velocity profiles inside the slit for $W = 0.4\,\text{mm}$ and $W = 0.8\,\text{mm}$, with $V_S = 6\,\text{m/s}$.

slit, resulting in a higher flow temperature, a higher flow velocity, and a higher velocity gradient, which disfavor flashback. Differently, for $W = 0.8\,\text{mm}$, the temperature at the center of the slit is close to the inlet flow temperature, resulting in a lower flow velocity and a lower velocity gradient, which promote flashback. At the same time, higher flow temperatures tend to increase the laminar flame speed, favoring flashback. These two effects influence the flame stabilization, but the former prevails resulting in the linear dependence of the flashback limits on the slit width under the conditions investigated in this study, as shown above.

We performed the same analysis for holes with different diameters W. In Figures 12 and 13, we show the burner plate temperature as a function of the velocity at the hole entry V_S and the flashback velocity as a function of the hole diameter W. For $W > 0.6\,\text{mm}$, we observe

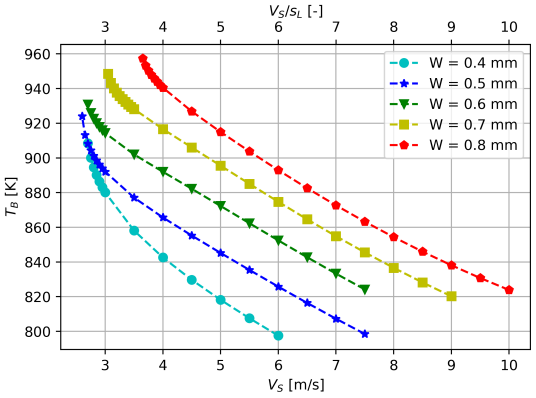

Figure 12: Burner plate temperature as a function of V_S for holes with different diameters W.

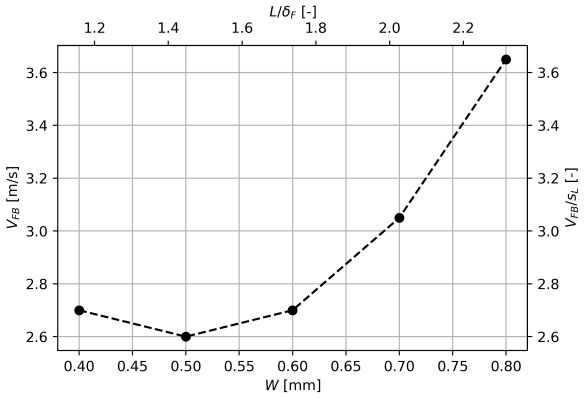

Figure 13: Flashback velocity as a function of the hole diameter W.

the flashback limits to increase when increasing the hole diameter. For $W < 0.6\,\text{mm}$, we observe a change in the trend, with the two competing effects described above counterbalancing each other for low diameters. The difference in the behaviors of flashback limits at low W for slits and holes could be related to a greater impact of heat losses to the burner for holes, and to preferential diffusion effects, but further investigation is needed for a complete understanding of the phenomenon.

Conclusions

In this work, we characterized the effects of the shape of the slits on the flashback limits of hydrogen premixed flames in multi-slit burners. We presented a steady-state methodology able to compute flashback velocities with a relatively low computational effort, and we validated it by means of a comparison with a transient approach. We investigated the effects of the slit length on the flashback limits, pointing out that, for sufficiently long slits, the flashback velocity is independent of the slit length. This is due to the fact that the flashback is initiated at the ends of the slits. For holes, we

observe lower burner plate temperatures, widening the flashback limits. Moreover, we analyzed the effects of the slit width on the flashback velocities, finding a linear correlation between the two quantities. For holes, the linear correlation between hole diameter and flashback velocity is lost, probably due to a greater importance of heat losses to the burner plate.

Acknowledgments

This research is supported by the Italian Ministry of University and Research (MUR) as part of the PON 2014-2020 "Research and Innovation" resources - Green/Innovation Action - DM MUR 1061/2021.

References

[1] EU Commission Press Release European Green Deal: the Commission proposes transformation of EU economy and society to meet climate ambitions (14 July 2021).

[2] H. de Vries, A. V. Mokhov, and H. B. Levinsky, The impact of natural gas/hydrogen mixtures on the performance of end-use equipment: Interchangeability analysis for domestic appliances, *Applied Energy* **208**, 1007 (2017).

[3] A. Aniello, T. Poinsot, L. Selle, and T. Schuller, Hydrogen substitution of natural-gas in premixed burners and implications for blow-off and flashback limits, *International Journal of Hydrogen Energy,* (2022), ISSN 0360-3199.

[4] H. Pers, A. Aniello, F. Morisseau, and T. Schuller, Autoignition-induced flashback in hydrogen-enriched laminar premixed burners, *International Journal of Hydrogen Energy* (2022), ISSN 0360-3199.

[5] F. Vance, L. de Goey, and J. van Oijen, Development of a flashback correlation for burner-stabilized hydrogen-air premixed flames, *Combustion and Flame* 112045 (2022), ISSN 0010-2180.

[6] Ansys Inc, Ansys Fluent 22.1 User's guide (2022).

[7] R. Bilger, S. Stårner, and R. Kee, On reduced mechanisms for methane-air combustion in non-premixed flames, *Combustion and Flame* **80**, 135 (1990).

[8] W. E. Stewart, Multicomponent mass transfer., *AIChE Journal* **41**, 202 (1995).

[9] H. J. Merk, The macroscopic equations for simultaneous heat and mass transfer in isotropic, continuous and closed systems, *Applied Scientific Research, Section A* **8**, 73 (1959), ISSN 1573-1987.

[10] K. Kuo, *Principles of Combustion* (Wiley, 2005), ISBN 9780471046899.

[11] M. F. Modest, in *Radiative Heat Transfer (Third Edition)*, edited by M. F. Modest (Academic Press, Boston, 2013), 541–584, third edition ed., ISBN 978-0-12-386944-9.